



**RESEARCH ARTICLE**

# Semi-synthetic degradable notochordal cell-derived matrix hydrogel for use in degenerated intervertebral discs: Initial in vitro characterization

Tara C. Schmitz<sup>1</sup>  | Bas van Genabeek<sup>2</sup>  | Maarten J. Pouderoijen<sup>2</sup> |  
 Henk M. Janssen<sup>2</sup> | Marina van Doeselaar<sup>1</sup> | João F. Crispim<sup>1</sup>  |  
 Marianna A. Tryfonidou<sup>3</sup>  | Keita Ito<sup>1</sup> 

<sup>1</sup>Orthopaedic Biomechanics, Department of Biomedical Engineering, Eindhoven University of Technology, Eindhoven, The Netherlands

<sup>2</sup>SyMO-Chem BV, Eindhoven, The Netherlands

<sup>3</sup>Department of Clinical Sciences of Companion Animals, Faculty of Veterinary Medicine, Utrecht University, Utrecht, The Netherlands

**Correspondence**

Keita Ito, Orthopaedic Biomechanics, Dept. Biomedical Engineering Eindhoven University of Technology GEM-Z 4.115, P.O. Box 513, 5600 MB Eindhoven, The Netherlands. Email: [k.ito@tue.nl](mailto:k.ito@tue.nl)

**Funding information**

the European Commission's Horizon 2020; iPSpine project, Grant/Award Number: 825925; Dutch Arthritis Society (LLP22)

**Abstract**

Low back pain is the leading cause of disability worldwide, but current therapeutic interventions are palliative or surgical in nature. Loss of notochordal cells (NCs) and degradation of the healthy matrix in the nucleus pulposus (NP), the central tissue of intervertebral discs (IVDs), has been associated with onset of degenerative disc changes. Recently, we established a protocol for decellularization of notochordal cell derived matrix (NCM) and found that it can provide regenerative cues to nucleus pulposus cells of the IVD. Here, we combined the biologically regenerative properties of decellularized NCM with the mechanical tunability of a poly(ethylene glycol) hydrogel to additionally address biomechanics in the degenerate IVD. We further introduced a hydrolysable PEG-diurethane crosslinker for slow degradation of the gels in vivo. The resulting hydrogels were tunable over a broad range of stiffness's (0.2 to 4.5 kPa), matching that of NC-rich and -poor NP tissues, respectively. Gels formed within 30 min, giving ample time for handling, and remained shear-thinning post-polymerization. Gels also slowly released dNCM over 28 days as measured by GAG effusion. Viability of encapsulated bone marrow stromal cells after extrusion through a needle remained high. Although encapsulated NCs stayed viable over two weeks, their metabolic activity decreased, and their phenotype was lost in physiological medium conditions in vitro. Overall, the obtained gels hold promise for application in degenerated IVDs but require further tuning for combined use with NCs.

**KEYWORDS**

biomaterial, intervertebral disc, notochordal cell-derived matrix, regeneration, restoration

**1 | INTRODUCTION**

Low back pain is one of the major causes of disability worldwide.<sup>1</sup> One possible cause is intervertebral disc (IVD) degeneration, which affects

the disc on both a biological and a biomechanical level: insufficient nutrition, loss of cells, and enhanced matrix degradation by nucleus pulposus cells (NPCs) cause a compressive load shift from the central nucleus pulposus (NP) to the annulus fibrosus (AF). This may result in AF tears under

This is an open access article under the terms of the [Creative Commons Attribution-NonCommercial](https://creativecommons.org/licenses/by-nc/4.0/) License, which permits use, distribution and reproduction in any medium, provided the original work is properly cited and is not used for commercial purposes.

© 2023 The Authors. *Journal of Biomedical Materials Research Part A* published by Wiley Periodicals LLC.

the new excessive stress, which in turn will induce vascular, neural and immunological invasion of the IVD and easier transport of noxious stimuli outward.<sup>2-5</sup> Clinical treatment options are lacking, and currently explored options include injectable cell carriers or filler materials, addressing either the need for biological regeneration in mildly degenerated IVDs, or restoring joint biomechanics in severe cases.<sup>6</sup>

Simultaneously addressing both biological regeneration and mechanical restoration of the degenerate IVD may be advantageous to address both short- and long-term treatment outcomes. Our group has previously shown that the use of notochordal cell-derived matrix (NCM) has regenerative effects *in vitro*<sup>7</sup> and *in vivo*,<sup>8</sup> and we further developed a simple decellularization protocol to yield decellularized NCM (dNCM) with similar bioactive properties to NCM.<sup>9</sup> However, NCM and dNCM behave more similarly to a thick viscous fluid and cannot bear physiological loads. Encapsulation of dNCM within a stiffer hydrogel thus presents an opportunity to combine both long-term biological and instant mechanical treatment approaches for disc regeneration.

Poly(ethylene glycol) (PEG) is a popular material for hydrogel formation within the field of regenerative medicine and tissue engineering, and has been previously used for materials intended for use in the NP.<sup>10</sup> However, PEG itself only slowly degrades, so degradable block-co-polymers and spacers have been described in literature to confer hydrolysable properties to PEG gels.<sup>11-13</sup> The degradation times of these polymers however is faster than the years-long tissue turnover within the NP.<sup>14</sup> For mechanical restoration approaches these materials would result in an initial improvement in joint biomechanics undermined by physiological loading onto incompletely regenerated tissue after premature biomaterial degradation. We here describe the synthesis of a novel degradable PEG-based crosslinker by introduction of urethane and thiol groups. Urethane groups have frequently been used in long-term drug release applications,<sup>15</sup> and thus may be useful in hydrogels delivering bioactive cargo to the NP. The thiol groups are reactive toward double bond groups, such as vinyl-sulfone groups, facilitating hydrogel formation through crosslinking.<sup>16</sup>

Additionally, cell transplantation has been heavily explored for IVD regeneration, as the residing NP cells may not be able to synthesize sufficient amounts of matrix for long-term joint mechanics restoration after biomaterial degradation. Notochordal cells (NCs) have been shown to exude regenerative effects through vesicle-derived growth factors and the specialized matrix they produce.<sup>17,18</sup> However, in humans, NC clusters within the disc start disappearing from young age.<sup>19</sup> New studies identified remnant NC and other progenitor cells potentially aiding the residing NPCs' matrix production after onset of disc degeneration.<sup>20,21</sup> However, animal-derived NCs are associated with several drawbacks when considering transplantation into humans, such as retroviral transmission.<sup>22</sup> Injection of for example, autologous induced pluripotent stem cell (iPSC)-derived NCs into the patient IVD may therefore present an avenue for further biological regeneration beyond administration of dNCM. Mesenchymal stromal cells have also been explored in this context.<sup>23,24</sup> NCs have previously been shown to be sensitive to substrate stiffness, preferring softer ones.<sup>25,26</sup> Gels designed for cell transplantation and biological regeneration of IVDs may therefore need to be softer than gels intended for purely mechanical restoration purposes.

Here, we investigate the capabilities of a tunable dNCM+PEG gel to assume stiffnesses of NC- rich matrices (porcine NP) or human NP, and to release dNCM from the respective gels. The approach presented here may be useful for both biological regeneration and mechanical restoration of IVDs of varying degeneration grades. We describe the material properties of these gels, the capacity of these hydrogels for cell injection into the disc in general, and for NC phenotype maintenance in particular.

## 2 | MATERIALS AND METHODS

Materials were obtained from Sigma Aldrich/Merck (Amsterdam, The Netherlands), unless stated otherwise.

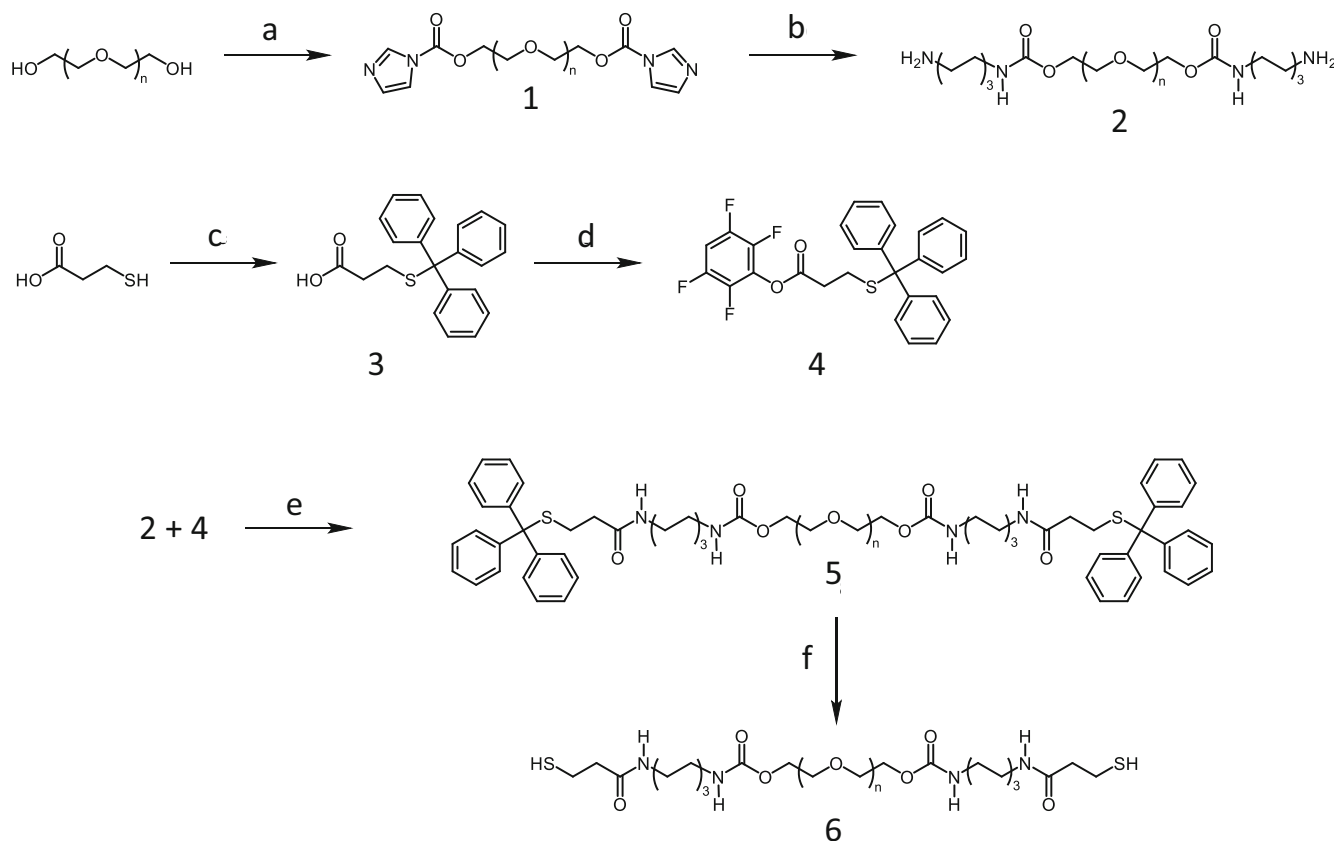
### 2.1 | Decellularization of NCM to obtain dNCM

Decellularized NCM (dNMC) was produced as published before.<sup>9</sup> Briefly, porcine spines (12 weeks old) were obtained from a local abattoir, according to local regulations. The IVDs were opened under aseptic conditions. NCM from 3 spines was pooled into one batch, briefly mixed with a sterile weighing spoon, and then aliquoted into 1–2 g tissue samples. Samples were frozen overnight at  $-80^{\circ}\text{C}$  before lyophilization for  $>72$  h at  $\leq -50^{\circ}\text{C}$  until completely dry. Decellularization was performed under aseptic conditions. Lyophilized NP tissue samples were treated with 200 U/mL benzonase in 50 mM Tris-HCl buffer, pH 7.5, 2.5 mM  $\text{MgCl}_2$  at 0.01 mL buffer/mg dry weight tissue for 48 h at  $37^{\circ}\text{C}$  on a roller at 2 rpm. Samples were then washed twice with 0.2 mL PBS/mg dry weight tissue for 30 min on a roller at 40 rpm. For easier buffer aspiration, samples were centrifuged at 1000g for 5 min. As much PBS as possible was removed in between washes and prior to freezing the samples and lyophilization for  $>72$  h until completely dry. dNCM was pulverized using a mortar and pestle/microdismembrator (Sartorius, Goettingen, Germany). Powders were UV-sterilized in a petri dish for  $2 \times 5$  min,  $1 \times 10$  min (stirring between) at 30 cm distance from a Philips TUVG30T8 UV lamp (Philips, Amsterdam, Netherlands).

### 2.2 | Synthesis and characterization of hydrolysable PEG-diurethane-dithiol crosslinker

The reaction scheme for the synthesis of the hydrolysable crosslinker is outlined in Reaction scheme 1. In the first step PEG (MW = 8000 g/mol) was activated using N,N'-carbodiimidazole (CDI) giving **1**. The activated PEG (**1**) was subsequently reacted with an excess of 1,6-diaminohexane; the product was purified using trituration in diethyl ether to give **2**.

The endcapper molecule **4** was synthesized by trityl protection of mercaptopropionic acid using trityl chloride in dichloromethane (DCM). After filtration and washing of the residue **3** was obtained. Thereafter, **3** was activated with 2,3,5,6-tetrafluorophenol using N,N'-diisopropylcarbodiimide (DIC) as coupling reagent. The product was purified via column chromatography yielding activated ester **4**.



**REACTION SCHEME 1** (A) *N,N'*-carbodiimidazole (CDI),  $\text{CHCl}_3$ , 1 h, RT, 96%; (B) 1,6-diaminohexane,  $\text{CHCl}_3$ , 2 h, 40°C, 97%; (C) tritylchloride, DCM, 1 h, RT, 100%; (D) 2,3,5,6-tetrafluorophenol, *N,N'*-diisopropylcarbodiimide (DIC), 4-(dimethylamino)pyridinium 4-methylbenzenesulfonate, tetrahydrofuran (THF), 0°C to RT, 1 h, 77%; (E) DCM, *N,N*-diisopropylethylamine (DIPEA), 72 h, RT, 92%; (F) 1,1,1,3,3,3-hexafluoroisopropan-2-ol (HFIP), boron trifluoride etherate, triethylsilane, 30 min, RT, 92%.

In the next step **2** and **4** were allowed to react in chloroform for 72 h at room temperature to yield **5**. Finally, the deprotection of **5** was performed using a mixture of 1,1,1,3,3,3-hexafluoroisopropan-2-ol, boron trifluoride etherate and triethylsilane. Purification was done by precipitating the product twice in diethyl ether to obtain **6** as a white powder.  $^1\text{H-NMR}$  and  $^{19}\text{F-NMR}$  spectral data as well as gel permeation chromatography (GPC; using dimethylformamide (DMF) eluent) data of **6** are compiled in the [Supplementary Information](#).

### 2.2.1 | Synthesis of poly(ethylene glycol)-bis(1*H*-imidazole-1-carboxylate) (**1**)

In a round-bottomed flask of 250 mL PEG (MW = 8000 g/mol, 32.6 g, 4.07 mmol, 1 moleq) was dried under vacuum and 120°C for 1 h. The material was dissolved in chloroform (100 mL) and was added via a syringe pump at 4 mL min<sup>-1</sup> to a solution of *N,N'*-carbodiimidazole (CDI, 5.28 g, 32.6 mmol, 8 moleq) in chloroform (70 mL). After addition of the PEG-solution, the reaction mixture was stirred for another hour at room temperature. The reaction mixture was triturated twice with diethyl ether, was filtrated, washed with ether and dried in vacuo at 40°C to give a white powder (32.1 g, 96%).

$^1\text{H NMR}$  (400 MHz, Chloroform-*d*)  $\delta$  8.16 (d,  $J = 1.1$  Hz, 2H), 7.45 (t,  $J = 1.5$  Hz, 2H), 7.07 (dd,  $J = 1.6, 0.9$  Hz, 2H), 4.59–4.53 (m, 4H), 3.87–3.79 (m, 4H), 3.64 (s, 819H).  $^{13}\text{C NMR}$  (101 MHz,  $\text{CDCl}_3$ )  $\delta$  137.2, 130.7, 117.2, 77.4, 77.3, 77.1, 76.8, 70.6, 68.6, 67.1. GPC: (DMF, PEG standards)  $M_n = 8.9$  kg/mol,  $M_w = 9.3$  kg/mol *polymer dispersity index* (PDI) = 1.04.

### 2.2.2 | Synthesis of poly(ethylene glycol)-bis(6-aminohexylcarbamate) (**2**)

In a flask of 250 mL **1** (32 g, 3.9 mmol, 1 moleq) was dissolved in chloroform (80 mL). This solution was added via a syringe pump at a speed of 4 mL/min to a solution of 1,6-diaminohexane (7.25 g, 62.4 mmol, 16 moleq) in chloroform (100 mL) at 40°C. After addition, the reaction mixture was stirred for another 2 h at 40°C. The reaction mixture was transferred to a round-bottomed flask of 3 L and was triturated twice with diethyl ether (1100 mL). The precipitate was filtered over a glass-fritted filter and the residue was washed twice with diethyl ether to give a white powder in a 97% yield (note: a small amount of dimerized product is formed).

$^1\text{H NMR}$  (400 MHz, Chloroform-*d*)  $\delta$  4.95 (s, 2H), 4.21 (t,  $J = 4.7$  Hz, 4H), 3.64 (s, 828H), 3.16 (q,  $J = 6.7$  Hz, 4H), 2.68 (t,  $J = 6.9$  Hz, 4H), 1.47 (m, 8H), 1.33 (m, 8H).  $^{13}\text{C NMR}$  (101 MHz,

$\text{CDCl}_3$ )  $\delta$  156.4, 72.8, 70.5, 69.6, 63.7, 42.1, 40.9, 33.6, 29.9, 26.5, 26.5. GPC (DMF, PEG standards) Peak 1:  $M_n = 15.6$  kg/mol,  $M_w = 15.9$  kg/mol,  $PDI = 1.02$ , Peak 2:  $M_n = 6.61$  kg/mol,  $M_w = 7.10$  kg/mol,  $PDI = 1.07$ .

### 2.2.3 | Synthesis of 3-(Tritylthio)propanoic acid (3)

To a solution of mercaptopropionic acid (1.2 g, 0.98 mL, 11.3 mmol, 1.0 moleq) in DCM was added (dropwise) a solution of trityl chloride (3.47 g, 12.4 mmol, 1.1 moleq) in DCM. The reaction mixture was stirred for 1 h at room temperature. The precipitated product was filtered, washed with diethyl ether and the residue was dried in vacuo at room temperature to obtain a white solid in quantitative yield.

$^1\text{H}$  NMR (400 MHz, DMSO- $d_6$ )  $\delta$  7.46–7.11 (m, 15H), 2.28 (t,  $J = 7.4$  Hz, 2H), 2.17 (t,  $J = 6.8$  Hz, 2H).  $^{13}\text{C}$  NMR (100 MHz, DMSO)  $\delta$  173.14, 144.85, 129.57, 128.50, 127.20, 66.66, 33.39, 27.17.

### 2.2.4 | Synthesis of 2,3,5,6-tetrafluorophenyl-3-(tritylthio)propanoate (4)

To a cooled (0°C) suspension of 3-(tritylthio)propanoic acid (3.94 g, 11.3 mmol, 1.0 moleq), 2,3,5,6-tetrafluorophenol (1.88 g, 11.3 mmol, 1.0 moleq) and 4-(dimethylamino)pyridinium 4-methylbenzenesulfonate (0.33 g, 1.13 mmol, 0.10 moleq) in tetrahydrofuran (THF) (16 mL) was added  $N,N'$ -diisopropylcarbodiimide (DIC, 1.57 g, 1.95 mL, 12.4 mmol, 1.10 moleq) in THF (2 mL). After addition the ice bath was removed, and the reaction mixture was stirred at room temperature for 1 h. Thereafter, the reaction mixture was diluted with heptane to give a white precipitate. The suspension was filtered, the residue was washed with heptane and the filtrate was concentrated in vacuo. The white solid residue was purified with column chromatography using mixtures of heptane/chloroform giving the pure product (4.33 g, 77%).

$^1\text{H}$  NMR (400 MHz, Chloroform- $d$ )  $\delta$  7.50–7.42 (m, 6H), 7.35–7.26 (m, 6H), 7.26–7.18 (m, 3H), 6.96 (tt,  $J = 9.9, 7.0$  Hz, 1H), 2.59 (t,  $J = 7.1$  Hz, 2H), 2.44 (t,  $J = 7.1$  Hz, 2H).  $^{13}\text{C}$  NMR (101 MHz,  $\text{CDCl}_3$ )  $\delta$  167.8, 147.2, 144.7, 144.4, 141.8, 139.3, 129.6, 128.0, 126.8, 103.2, 67.1, 32.8, 26.4.

### 2.2.5 | Synthesis of poly(ethylene glycol)-bis(6-(3-(tritylthio)propanamido)hexyl)carbamate (5)

To a solution of **2** (2.13 g, 0.26 mmol, 1.00 moleq) in DCM (9 mL) was added 2,3,5,6-tetrafluorophenyl 3-(tritylthio)propanoate **4** (1.28 g, 2.6 mmol, 10.0 moleq) and  $N,N$ -diisopropylethylamine (DIPEA, 0.40 g, 0.54 mL, 3.09 mmol, 12.0 moleq). The reaction mixture was stirred at room temperature for 72 h. After 72 h the reaction mixture was precipitated twice in diethyl ether, filtrated, washed with diethyl ether and dried in vacuo at 40°C to give a white powder (2.1 g, 92%).

$^1\text{H}$  NMR (400 MHz, Chloroform- $d$ )  $\delta$  7.50–7.36 (m, 12H), 7.28 (m, 12H), 7.24–7.16 (m, 6H), 5.41 (s, 2H), 4.84 (s, 2H), 4.20

(t,  $J = 4.7$  Hz, 4H), 3.64 (s, 745H), 3.14 (dq,  $J = 12.6, 6.6$  Hz, 8H), 2.49 (t,  $J = 7.3$  Hz, 4H), 2.02 (t,  $J = 7.3$  Hz, 3H), 1.45 (m, 8H), 1.30 (q,  $J = 3.7$  Hz, 8H). GPC (DMF, poly(ethylene glycol) standards) Peak 1:  $M_n = 18.3$  kg/mol,  $M_w = 18.5$  kg/mol,  $PDI = 1.02$ , Peak 2:  $M_n = 9.2$  kg/mol,  $M_w = 9.6$  kg/mol,  $PDI = 1.04$ .

### 2.2.6 | Synthesis of poly(ethylene glycol)-bis(6-(3-thiopropanamido)hexyl)carbamate (PEG-diurethane-dithiol) (6)

To a stirring cleavage cocktail consisting of 1,1,1,3,3,3-hexafluoroisopropanol (22 mL), boron trifluoride etherate (55  $\mu\text{L}$ ), triethylsilane (1.3 mL) was added **5** (1.97 g, 0.22 mmol, 1.0 moleq). After 30 minutes at room temperature the reaction mixture was precipitated in diethyl ether (350 mL). The residue was filtered through a glass fritted filter and washed with ether. The solid was redissolved in chloroform and precipitated a second time in diethyl ether (as described above) and was dried in vacuo giving a white powder (1.72 g, 92%).

$^1\text{H}$  NMR (400 MHz, Chloroform- $d$ )  $\delta$  5.79 (s, 2H), 4.91 (s, 2H), 4.21 (t,  $J = 4.7$  Hz, 4H), 3.64 (s, 836H), 3.26 (q,  $J = 6.7$  Hz, 4H), 3.16 (q,  $J = 6.6$  Hz, 4H), 2.82 (dt,  $J = 8.4, 6.7$  Hz, 4H), 2.48 (t,  $J = 6.7$  Hz, 4H), 1.62 (t,  $J = 8.3$  Hz, 2H), 1.58–1.42 (m, 8H), 1.42–1.26 (m, 8H).  $^{13}\text{C}$  NMR (101 MHz,  $\text{CDCl}_3$ )  $\delta$  170.6, 156.5, 70.6, 69.7, 63.8, 40.6, 40.4, 39.2, 29.8, 29.4, 26.0, 20.5. GPC: Peak 1:  $M_n = 19.0$  kg/mol,  $M_w = 19.9$  kg/mol,  $PDI = 1.05$ , Peak 2:  $M_n = 8.5$  kg/mol,  $M_w = 9.0$  kg/mol,  $PDI = 1.06$ .

## 2.3 | Encapsulation of dNCM in a tunable PEG gel

PEG-gels containing dNCM were prepared by reacting the PEG-diurethane-dithiol crosslinker with 8-arm-PEG-vinyl sulfone while in the presence of dNCM. Accordingly, dNCM powder was reconstituted to 5% w/v in PBS and homogenized by passing through increasing needle gauge (G) sizes up to 27 G. The dNCM suspension was centrifuged for 5 min at 300g before use. 8-arm-PEG-vinyl sulfone (JenKem, Plano, Texas) was dissolved to 250 mg  $\text{mL}^{-1}$  in PBS. The PEG-diurethane-dithiol crosslinker was dissolved to 212.5 mg  $\text{mL}^{-1}$  in PBS. The components were then mixed as described in Table 1 to yield stiff and soft gels. One batch of dNCM was used for all gel preparations. Rheological and gelation properties of dNCM-PEG gels Soft and stiff dNCM-PEG gels (all  $n = 3$ ) were measured in a parallel platen configuration (0.05 N preload, diameter 8 mm), at 37°C with a rheometer (Ares 3000, TA instruments, Assen, Belgium). First a frequency sweep (0.1 to 100 rad/s, at 1% strain), then a strain sweep (0.1% to 100%, at 1 rad/s) was performed. Gelation was measured at 1% strain, 1 rad/s for 30 min at 37°C.

## 2.4 | Gel swelling & component leaching

Stiff and soft gels were incubated in media mimicking the healthy and degenerate IVD environment (adapted from Thorpe et al.<sup>27</sup>).

The media composition is detailed in Table 2. The pH is at 7.1 for the healthy and 6.8 for the degenerate IVD environment at 5% CO<sub>2</sub> in the incubator. Gels were incubated for 4 weeks, and the media changed twice per week. GAG content was assayed from the supernatant with DMMB assay<sup>28</sup>; empty gels were used as negative controls. Relative GAG loss was calculated from mean GAG amount per mg dNCM as determined before.<sup>9</sup> Gels were weighed gravimetrically and swelling determined relative to original weight:

$$\text{swelling} = \frac{(m_t - m_0)}{m_0} \times 100\%, \quad (1)$$

with  $m_t$ , wet weight at timepoint  $t$ , and  $m_0$ , initial wet weight.

## 2.5 | dNCM distribution within gels

Soft and stiff gels with and without dNCM were prepared as described above. In gels without dNCM, the respective dNCM-volume was replaced by PBS. Gels were embedded in TissueTek (Sakura, Finetek USA, Torrance) and frozen on dry ice. Cryosections were prepared on a cryotome (CM1950, Leica, Amsterdam, The Netherlands) with 50  $\mu\text{m}$  thickness. Sections were stained with Alcian Blue to visualize dNCM.

**TABLE 1** Composition of stiff and soft dNCM-PEG gels.

Component	Stiff gel	Soft gel
8-arm PEG-vinyl sulfone	5% w/v = 2.5 mM	5% w/v = 2.5 mM
Linear PEG-diurethane-dithiol crosslinker	8.5% w/v = 10 mM	2.125% w/v = 2.5 mM
Vinyl sulfone: thiol molecular ratio	1:1	1:0.25 (4:1)
dNCM	2% w/v	2% w/v
Total solid content	15.5% w/v	9.125% w/v

**TABLE 2** Composition of healthy and degenerate disc environment-mimicking medium.

Component	Healthy disc environment-mimicking medium	Degenerate disc environment-mimicking medium	Supplier
Low glucose DMEM	4.99 g/500 mL	4.99 g/500 mL	Gibco
Sodium bicarbonate	0.425 g/500 mL	0.213 g/500 mL	Sigma
N-Methyl-Glucamine HCl (NaCl homolog for adjusting medium osmolarity)	92.5 mmol/L (450 mOsm/kg)	47.5 mmol/L (350 mOsm/kg)	Sigma
Penicillin/Streptomycin	1% v/v	1% v/v	Gibco
L-ascorbic acid	25 $\mu\text{g}/\text{mL}$	25 $\mu\text{g}/\text{mL}$	Gibco
L-glutamine	1% v/v	1% v/v	Gibco
ITS-X	1% v/v	1% v/v	Gibco
L-Proline	40 $\mu\text{g}/\text{mL}$	40 $\mu\text{g}/\text{mL}$	Sigma
Albumax	1.25 mg/mL	1.25 mg/mL	Gibco

## 2.6 | Injectability of MSCs within the dNCM + PEG gels

Injectability testing was conducted with human bone marrow-derived mesenchymal stromal cells (MSCs) (Lonza, Cohasset).<sup>29</sup> MSCs are the most commonly used cell investigated for intervertebral disc regeneration,<sup>30</sup> and were used in our injectability test for this reason, and as a generic cell type standing in for any other cell type of interest in the field as published before.<sup>9</sup> MSCs were cultured in high glucose DMEM (hgDMEM) supplemented with 10% FBS (Bovogen Biologicals, Melbourne, Australia), 1% Penicillin/Streptomycin, 1% non-essential amino acids, and 1 ng/mL basic fibroblast growth factor (bFGF, Peprotech, Hamburg, Germany) and passage 6 was used for the experiment. Cells were resuspended in 5% w/v dNCM and then mixed with the polymers to encapsulate them within the gels (50  $\mu\text{L}/\text{sample}$ ). Gels were aspirated into a syringe through a 16G needle, and ejected through a 27G needle. Afterwards cells were cultured for 24 h in hgDMEM (Gibco, Landsmeer, The Netherlands) with 10% FBS (Gibco), 1% penicillin/streptomycin. A LIVE/DEAD staining with Calcein-AM/Propidium Iodide (1 and 10  $\mu\text{g}/\text{mL}$ , respectively) (Invitrogen, Fisher Scientific, Landsmeer, Netherlands) for 1 h in serum-free hgDMEM was performed. Images were acquired on an Apotome microscope (Zeiss, Jena, Germany). Samples were prepared in triplicate, with at least two images acquired per sample. Cell viability was quantified using ImageJ. Viabilities >70% were determined as acceptable in line with FDA regulations.<sup>31</sup>

## 2.7 | Encapsulation of porcine notochordal cells within dNCM-PEG gels & culture

Porcine NCs were isolated from 12-week-old spines as previously described. Briefly, spines were cleaned, disinfected and opened aseptically to isolate the NP tissue. The NP tissue was then digested in 0.1% w/v pronase for 30 min before digestion in 0.1% w/v collagenase overnight. Digested NP tissue was then strained through a 70  $\mu\text{m}$  cell strainer and NCs counted with a NucleoCounter<sup>®</sup> NC-



200™ (Chemometec, Allerød, Denmark). Gels with and without dNCM were prepared as follows: NCs were resuspended in 5% w/v dNCM or PBS before final mixing with PEG-vinyl sulfone and PEG-diurethane-dithiol for gel formation with a final cell concentration of  $4 \times 10^6$  cells/mL. Gels of 50  $\mu$ L were polymerized for 1 h at RT. Gels were cultured in healthy-disc-like media in a 96-well plate. Media osmolarity was adjusted to 450 mOsm by dissolving N-methyl-glucamine HCl in the medium as described above. Medium was refreshed every 2 days, and supernatant kept for a lactate assay on metabolic activity. At day 14, gels were cut in half for both, histological stainings and DNA measurements from the same sample as described below.

## 2.8 | DNA measurements

Gels were lyophilized for >48 h until completely dry and their dry weight recorded. Gels were then digested overnight at 60°C using 140 mg/mL papain in 100 mM phosphate buffer, 5 mM L-cysteine, 5 mM EDTA. Gels were then frozen at -20°C for >24 h, before thawing and mincing with plastic “mini-pestles” within the digestion solution. Samples were vortexed and left at room temperature undisturbed for 10 min to allow for sinking of PEG gel fragments and easy aspiration of the supernatant. The supernatant's DNA concentration was determined using the Qubit DNA assay (Qubit dsDNA HS assay, Thermo-Fisher Scientific, Landsmeer, The Netherlands) following the manufacturer's instructions.

## 2.9 | Lactate assay for measuring metabolic activity

Lactate in medium supernatant was measured as previously published.<sup>32</sup> Briefly, 40  $\mu$ L of 1:8–1:64 diluted medium supernatants and sodium L-lactate standards (0–1 mM) were mixed with a solution of 5 mg/mL  $\beta$ -nicotinamide adenine dinucleotide, 0.2 M glycine buffer and 22.25 U/mL L-lactate dehydrogenase and incubated at 37°C for 30 min before reading absorbance at 340 nm (Synergy HTX, BioTek, Winooski). Lactate readings were normalized to median DNA amount at D0 for the respective gel group. Note that the first possible timepoint for lactate measurement is at day 2 (first medium change), since at day 0 cells did not have time to metabolize the glucose within the medium and lactate readout would be 0.

## 2.10 | Histological staining

Gels at D0 and D14 were fixed overnight in 3.7% formalin, and afterwards dehydrated and embedded into paraffin. 10  $\mu$ m sections were cut with a cryotome (Leica), before staining with Hematoxylin and Eosin for nuclei and cytoplasmic staining, respectively. Images were acquired in brightfield microscopy (Axiovert Observer Z31, Zeiss).

## 2.11 | Statistics

Differences in released dNCM amounts from gels were investigated using a Kruskal-Wallis test with Dunn Post-hoc testing employing a Bonferroni correction. Differences in DNA amounts in gels with encapsulated NCs were investigated with a three-factor ANOVA (dNCM presence, stiffness, time) with Tukey's post-hoc correction in R (v3.6.3). Significance levels were set at  $p < .05$ .

## 3 | RESULTS

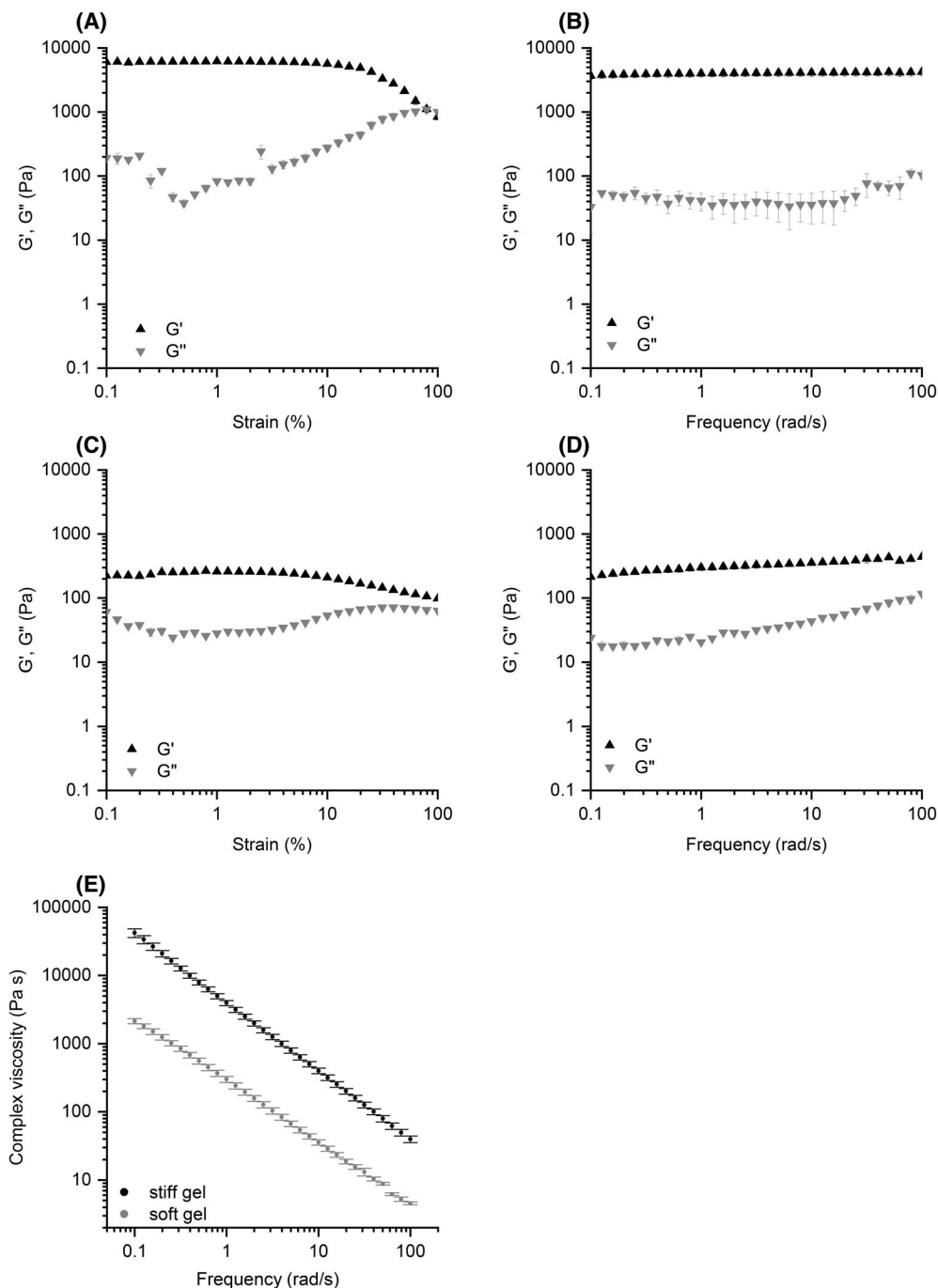
By varying the crosslinker amount within the gels we obtained two gels with stiffnesses that differed in one order of magnitude: the stiffer gel exhibited a median complex modulus of 4508 Pa at 10% strain, whereas the softer gel with less crosslinker displayed a median complex modulus of 174 Pa (Figure 1A,C). The crossover points for  $G'' > G'$  were  $> > 11\%$  strain in both gels (Figure 1A,C), that is, in supraphysiological strain values for the degenerated disc.<sup>33</sup> With increasing shear frequency, the gels' shear moduli slightly increased (Figure 1B,D). Overall, gels formed within 30 min (Figure 2) and were shear-thinning post-polymerization as viscosity decreased with increasing shear rate (Figure 1E).

Further, both gel types swelled up to 150% relative to their initial wet weight independent of healthy or degenerate IVD-like medium conditions (Figure 3A,B). Stiff gels swelled within 24 h to 100% of initial wet weight, and maintained their swollen weight for 28 days. Soft gels seemed to continuously swell over the 28-day time period reaching 150% initial wet weight by the end of the culture period.

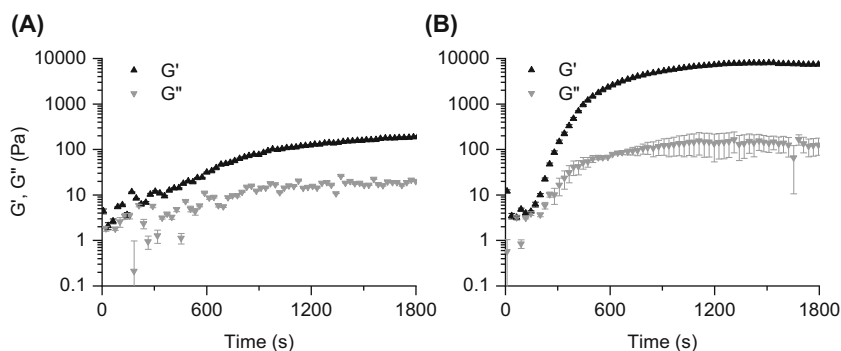
To confer bioactive and regenerative properties to the gels in addition to their mechanical tunability, we encapsulated decellularized NCM (dNCM) as cargo within the gels. By simple homogenization via pipetting, we obtained an even distribution of dNCM within both the stiff and soft gel as demonstrated by an Alcian Blue staining of gels (Figure 3C). Gels without encapsulated dNCM did not exhibit any stain, indicating that PEG does not react with the Alcian Blue dye. We also observed that the gels permitted slow effusion of dNCM into its surroundings; (d)NCM consists largely of glycosaminoglycans (GAGs)<sup>9</sup> and we measured their release into media as a proxy for dNCM release. dNCM effusion seemed to be gel- and media-dependent, where soft gels in general “lost” the encapsulated dNCM quicker than their stiff counterparts, and media mimicking the degenerate IVD-environment displayed larger amounts of released GAGs over time (Figure 3D,E). Loss of dNCM is highest within the first 2 days, after which release into the surrounding media slows down. According to median GAG content of dNCM<sup>9</sup> encapsulated in the gels, soft gels lost  $\approx 75\%$  of dNCM in healthy IVD-like conditions, but all of the encapsulated dNCM in degenerate IVD-like IVD conditions ( $\approx 125\%$ ). Contrary to this, stiff gels leached only up to  $\approx 25\%$  of their dNCM cargo in degenerate or healthy IVD-like medium.

For any cell-transplantation-based approach, cells must remain viable after injection of the gel into the NP. Here, we opted for using

**FIGURE 1** (A,C) Strain sweeps of stiff and soft dNCM + PEG gels, respectively. (B,D) Frequency sweeps of stiff and soft dNCM + PEG gels, respectively. (E) Viscosity reduces with increasing shear even after full polymerization of gels. All  $n = 3$ , average  $\pm$  standard error of the mean (SEM) plotted.



**FIGURE 2** Gelation of (A) soft and (B) stiff dNCM + PEG gels. All  $n = 3$ , average  $\pm$  SEM plotted.



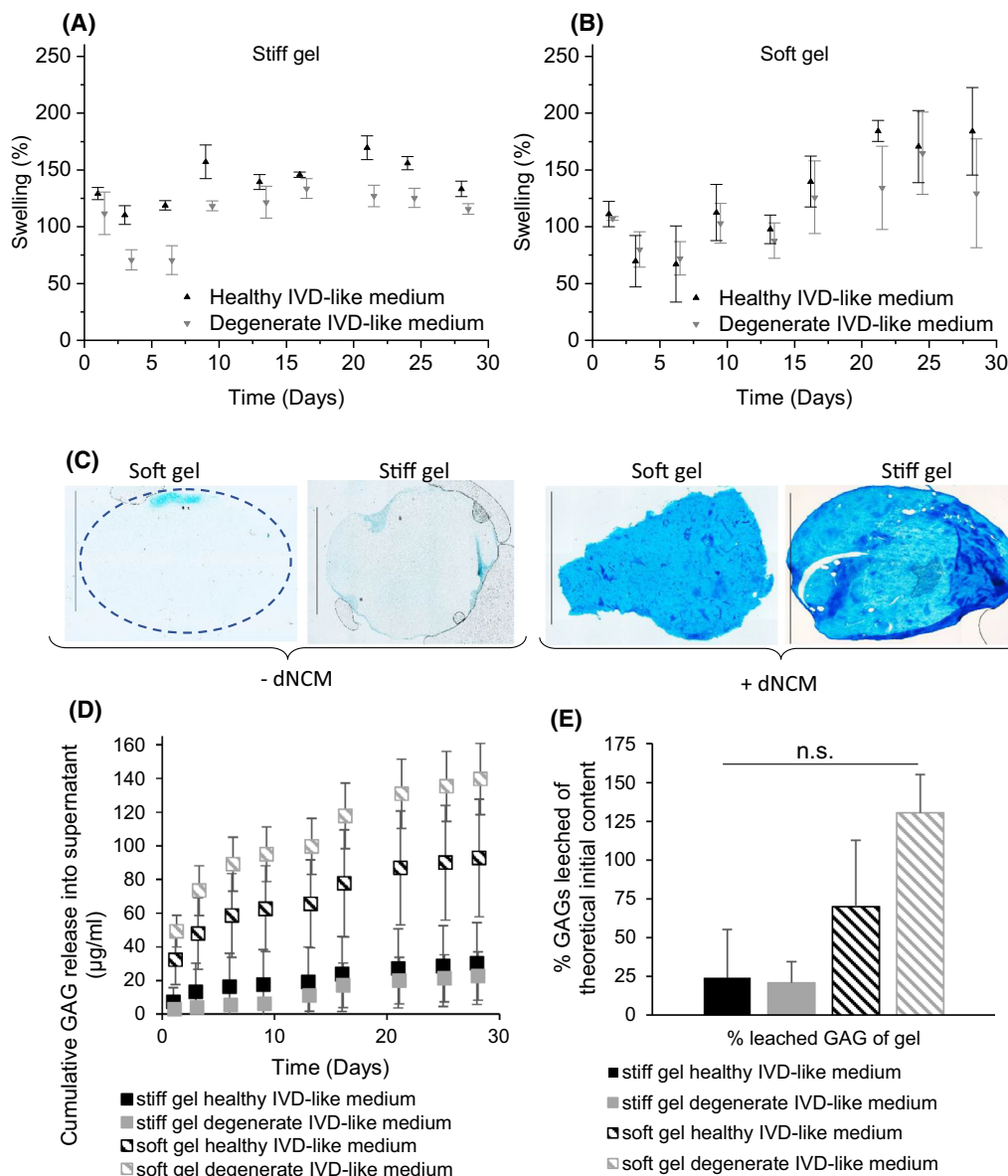


**FIGURE 3** (A, B) Swelling behavior of stiff & soft gels relative to initial gel wet weight over time. (C) dNCM distribution within gels visualized by Alcian Blue staining. Scale bar: 5 mm. (D, E) dNCM-release approximated by GAG-release into supernatant over time depends on gel formulation and medium conditions. All  $n = 3 \pm$  SEM.

MSCs as a stand-in for any cell type of interest to evaluate survival after extrusion through a 27 G needle: MSC viability post-injection remained high at >80% median viability (Figure 4A), with stiffer gels trending toward lower viability values overall. DNA content after NC encapsulation remained stable for soft gels and stiff gels with dNCM over 14 days while lactate content in the medium decreased over 2 weeks in culture for all culture groups (Figure 4B,C). Initial lactate content in the medium was highest for soft gels with and without dNCM, and did not reach zero for these groups over 14 days. Medium lactate content for stiff gel groups was only detectable for  $\approx 10$  days. NC morphology is characterized by the overall large cell size and presence of large vacuole.<sup>18</sup> These can be observed in native porcine NP sections and for some cells after NC isolation from porcine NP tissue.

Overall, the encapsulated cells lost their characteristic NC morphology including their vacuoles, and the cells shrunk in size (Figure 4D). For stiff gels without dNCM, few cells were visible, corroborating the lower DNA amount measured for this group at D14 (Figure 4B) and supplementary Figures 1-3.

## 4 | DISCUSSION

Within the scope of this article, we conceptualized a tunable hydrogel approach to satisfy both biological and mechanical need for IVD regeneration and restoration. Regeneration of the NP through cell-mediated novel matrix deposition may benefit early degenerated



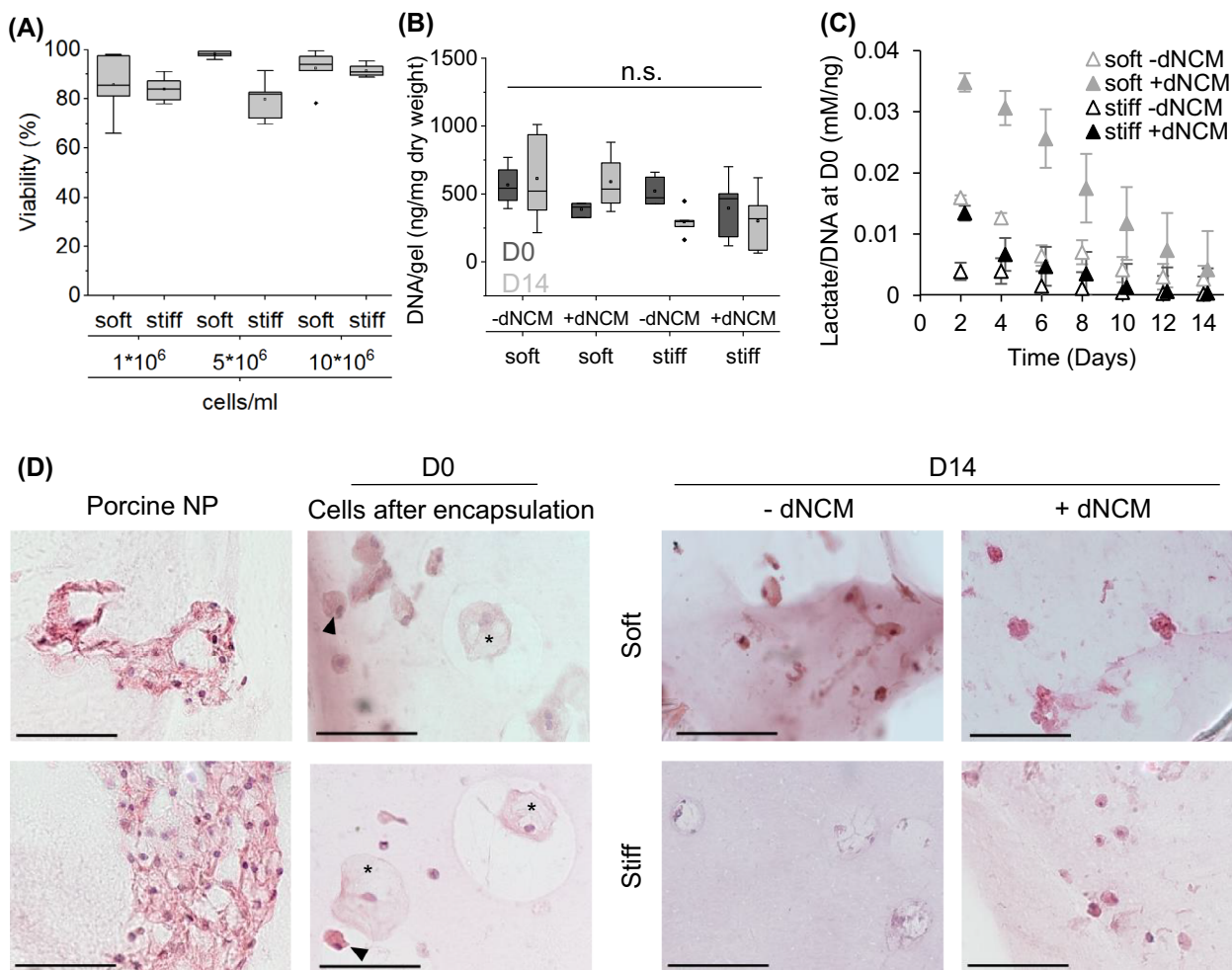


**FIGURE 4** (A) MSC viability post-extrusion through a 27 gauge needle remains high (acceptable viability level was set at 70%). (B) DNA content of encapsulated NCs stays constant in all gels except stiff gels without dNCM. All  $n = 5$ . (C) Lactate production of cells decreases with culturing time. All  $n = 5$ , average  $\pm$  SEM plotted. (D) NC morphology in porcine NP (two images shown for reference), after encapsulating in PEG gels (stiff gels - dNCM as example shown here) and after 14 days culture in the respective gel groups. NCs were encapsulated as single cells. Cells with (\*) and without vacuoles (arrowheads) can be seen at D0, while at D14 only small round cells remain. Scale bar: 50  $\mu$ m.

IVDs, whereas a mechanical restoration may take priority for more advanced degenerated IVDs. A multitude of biomaterials have previously been developed for use in the IVD - one popular base material for biomaterials for the IVD (and biomaterials in general) is PEG due to its tune ability and biocompatibility. Several injectable PEG-based hydrogels have also been approved by the FDA for various use cases, but none for the IVD so far.<sup>34</sup>

We chose to modify our PEG gels' stiffness by varying the crosslinker concentration to address different therapeutic needs depending on degeneration state of the IVD and its ability to deliver cells. The resulting gels range from 0.2 to 5 kPa in shear stiffness, covering the reported range of NC-rich porcine<sup>35</sup> and human NP stiffness.<sup>36,37</sup> Importantly, crossover points for  $G'$  and  $G''$  were  $> > 11\%$  strain for both gels and therefore exceeds the reported range for degenerated IVDs.<sup>33</sup> Both gels swell up to 150% of initial wet weight in free swelling conditions. The soft gel seems to continuously swell over the 28-day period, potentially due to crosslink-degradation. Swelling is

one of the hallmarks of healthy NP tissue and IVD joint mechanics.<sup>38</sup> With their swelling potential both gels may restore swelling pressure of the disc (assuming an intact annulus fibrosus), and therefore biomechanical joint function. Additionally, the stiff gel can assume stiffnesses close to that of the intended target tissue within the disc as mentioned above, and therefore may aid in biomechanical restoration of the joint in its non-swollen state.

The employed crosslinker was chosen to mimic slow degradation under physiological conditions to promote a slow replacement of hydrogel with newly deposited matrix within the IVD, as NP matrix turnover takes months to years.<sup>14,39</sup> Urethanes have been widely reported in sustained drug release applications<sup>15</sup> as their degradation is driven by hydrolysis and relatively slow.<sup>40</sup> Within the timeframe examined here, no degradation of the gels was found. Note that urethane degradation leads to  $\text{CO}_2$  release.<sup>41,42</sup>  $\text{CO}_2$  may dissolve in the surrounding water-rich disc tissue after implantation, and hypothetically affect disc tissue pH through hydration into  $\text{H}_2\text{CO}_3$ , and

subsequent decomposition into  $H^+$  and  $HCO_3^-$ . However, due to the long degradation timeframe and thereby low  $CO_2$  concentration at any one timepoint, as well as carbonic anhydrase production by mature NP cells routinely employing  $CO_2$  and  $HCO_3^-/H^+$  for acid-base buffering,<sup>43,44</sup> the effect of  $CO_2$  release from the gel onto local disc pH is expected to be tolerable. Further studies on the hydrolysable PEG-crosslinker degradation would be beneficial to fully characterize the gel presented here. A study by Jia et al. found no degradation of their PEG-polyurethane hydrogels over 28 days,<sup>45</sup> indicating that also in our case gel degradation over the studied period is unlikely. A future improvement on our gel concept could see the use of ester-based degradable PEGs, but their degradation time frame still ranges in the weeks<sup>13</sup> rather than months. Substituting for a poly ( $\epsilon$ -caprolactone)-based<sup>46</sup> or peptide-based<sup>47–49</sup> crosslinker could also be envisioned, but may affect mechanical and swelling properties adversely.

In terms of clinical usability, the gel formulation provides ample time for preparation and injection into the disc: gels formed within 10 min at neutral pH after mixing of all components and were stably polymerized at 30 min. A dual syringe may be used if the envisaged handling & injection time exceeds 10 min to delay component mixing and circumvent injection difficulty (although fully formed gels are also shear-thinning, i.e., injectable). Additionally, vinyl sulfone-thiol reactions are pH dependent, and take longer with decreasing pH such as found in the disc.<sup>50</sup> In situ gelation within the disc is therefore expected to take longer than described here due to lowered pH in the degenerated disc: at pH 6.6 (lower than what is expected in the degenerated disc), gelation in thiol-vinyl sulfone-crosslinking-based hydrogels is  $\approx 10\times$  slower compared to neutral pH.<sup>51,52</sup> Clinically, patients would therefore need to restrict their movement as much as possible for circa 5 h after administration of the gels described in our study to prevent leakage after injection.

While the PEG confers mechanical tunability and the PEG-urethane crosslinker degradability, the encapsulated dNCM serves as bioactive cargo in two ways: it provides cell attachment sites through its collagen content, and also harbors bioactive factors, which may act on the resident IVD cells. dNCM's anabolic effect onto NPCs was recently demonstrated by us<sup>9</sup> and its release from the PEG-based hydrogel may serve as a long-acting therapeutic intervention. Within our gels, vinyl sulfone may react with accessible thiol groups on proteins present in dNCM, thereby slowing release of bioactive factors and potentially diminishing their effect especially with soft gels where more free vinyl sulfone groups are present.<sup>53</sup> To elucidate the remaining bioactive effect of the encapsulated dNCM, future ex vivo or in vivo studies are therefore needed.

In free swelling conditions, dNCM release was quicker from soft gels compared to stiff gels. This can be explained by a smaller hydrogel mesh size (i.e., space between PEG-chains) for the stiff gels due to their higher crosslinker amount, which limits diffusion (especially for large molecular weight molecules, such as GAGs as found in dNCM). Similarly, higher crosslinking density may explain the slightly lower swelling ratio of stiff gels compared to soft ones.<sup>54</sup> Interestingly, swelling was not affected by osmolarity or pH of the culture medium

mimicking either healthy or degenerate disc conditions. This indicates that gel swelling is mainly driven by interaction of water directly with the gels' PEG backbone.<sup>55</sup> Maintenance of the swollen gel weight over time despite dNCM effusion also agrees with this. Notably, release of dNCM from gels may result in decreasing gel stiffness over time in vivo, which may diminish the mechanical restoration facilitated by the stiff gel. dNCM-mediated proliferation and matrix production by disc cells however may off-set this loss in gel stiffness. Nevertheless, long-term animal studies in an appropriate model will be necessary to elucidate the fate of the proposed gels and their long-term effect onto disc mechanics.

In this study, we further investigated the potential of dNCM-containing PEG gels for cell injection in general, and retaining NC phenotype in particular. One of the most popular choices for cell-mediated disc regeneration is usage of human mesenchymal stromal cells (MSCs) in both preclinical<sup>30</sup> and clinical studies.<sup>6</sup> In line with this, we here demonstrate viability  $>80\%$  of MSCs encapsulated within dNCM+PEG gel formulations at different concentrations post-extrusion through a 27 G needle, rendering this a viable future research avenue.

NCs have been investigated for their growth-factor containing vesicles and their use in regenerative medicine, especially the IVD field.<sup>18,56,57</sup> Here, we encapsulated NCs to examine their further use in cell transplantation in the tunable dNCM+PEG gels for additional biological regeneration of the disc. Based on the DNA content measured per gel, NCs may survive better in softer gels compared to stiffer gels, where dNCM may have a slight compensatory effect over the two week culture time. Contrary to DNA measurements, lactic acid within the medium supernatant decreases over time, indicating cessation of metabolic activity. NCs are known for their sensitivity in vitro, and optimized cell-culture setups have been established specifically for retaining NC phenotype, but these do not reflect the in situ conditions we examined here. It is also known that NCs lose their phenotype on stiff substrates quicker compared to soft ones,<sup>25,26</sup> and lose their phenotype when encapsulated.<sup>58</sup> In general cells tend to prefer encapsulation within softer gels compared to stiffer ones with high macromere content.<sup>59</sup> Currently, there is no consensus on definitive NC and NPC markers for for example, quantitative polymerase chain reaction or immunohistochemistry stainings, hindering a straight-forward characterization of our cells at D14.<sup>60</sup> The overall loss of vacuoles however points to a loss of NC phenotype and potential differentiation toward NPC-like cells. In the context of disc regeneration strategies this might imply that no anabolic growth factors would be released by the encapsulated cells to act on resident IVD cells. Longer culturing time frames could detect potential matrix deposition by the encapsulated cells, which at D14 is expected to be minimal (also considering their metabolic activity found in this study). Further improvements on NC phenotype retention within our gels could see the encapsulation of NC clusters, not single cells, as this has been found to be beneficial for NC survival and phenotype maintenance.<sup>61,62</sup> Their effect onto in situ IVD cells will need to be assessed in upcoming ex vivo/in vivo trials. For clinical translation, a further investigation into iPSC-derived NC- or NPC-fate within our gels

would be beneficial, as patient-derived reprogrammed NCs/NPCs present a new avenue for cell-mediated IVD regeneration. Previously published protocols however are low in yield,<sup>63,64</sup> which is why we opted for using primary NCs as an attainable alternative. Porcine NCM has been reported to increase NC-markers in iPSC-derived NC-like cells<sup>65</sup>; an encapsulation within our soft dNCM + PEG gel may therefore be a novel approach for tackling early disc degeneration. Extensive phenotypic and functional characterization of the iPSC-derived NCs for extended period of culture within the gels and in explant culture models are needed to demonstrate the potential of the developed dNCM+PEG gels.

## 5 | CONCLUSION

With the approach developed here, potentially patient groups with either early or late IVD degeneration may be satisfied with our tunable hydrogel system. By varying the concentration of crosslinker within our gel, we may obtain gels with a wide range of stiffnesses suitable for either injection and cargo/cell delivery into the disc for biological regeneration, or mechanical restoration via PEG-swelling and overall gel stiffness.

### AUTHOR CONTRIBUTIONS

Tara C. Schmitz: conceptualization, data curation, formal analysis, investigation, methodology, validation, writing original draft, visualization.

Henk M. Janssen: conceptualization, formal analysis.

Maarten J. Pouderoijen and Bas van Genabeek: synthesis, purification and analysis of PEG-diurethane-dithiol crosslinker.

Marina van Doeselaar: methodology, formal analysis, review & editing draft.

João F. Crispim: supervision, review & editing draft.

Marianna A. Tryfonidou: funding acquisition, project administration, supervision, resources, review & editing draft.

Keita Ito: conceptualization, funding acquisition, project administration, supervision, resources, review & editing draft.

### ACKNOWLEDGMENTS

We would like to thank Jurgen Bulsink for his skills in mold-preparation for hydrogel curing, and Roos Cardinaels for contributing her expertise on rheology data analysis.

### FUNDING INFORMATION

This work was supported by the European Commission's Horizon 2020 funding program for the iPSpine project [grant number 825925]. MAT receives funding from the Dutch Arthritis Society (LLP22).

### CONFLICT OF INTEREST STATEMENT

K.I. is CSO of NC Biomatrix, a company developing dNCM as a commercial product, which holds a license to the IP for its production process [United States Patent Application 20190022278].

### DATA AVAILABILITY STATEMENT

The data that support the findings of this study are available from the corresponding author upon reasonable request.

### ORCID

Tara C. Schmitz  <https://orcid.org/0000-0003-4247-1620>

Bas van Genabeek  <https://orcid.org/0000-0002-4516-4469>

João F. Crispim  <https://orcid.org/0000-0001-6818-6401>

Marianna A. Tryfonidou  <https://orcid.org/0000-0002-2333-7162>

Keita Ito  <https://orcid.org/0000-0002-7372-4072>

### REFERENCES

- Maher C, Underwood M, Buchbinder R. Non-specific low Back pain. *Lancet*. 2017;389(10070):736-747. doi:10.1016/S0140-6736(16)30970-9
- Humzah MD, Soames RW. Human intervertebral disc: structure and function. *Anat Rec*. 1988;220(4):337-356. doi:10.1002/ar.1092200402
- Wong J, Sampson SL, Bell-Briones H, et al. Nutrient supply and nucleus pulposus cell function: effects of the transport properties of the cartilage endplate and potential implications for intradiscal biologic therapy. *Osteoarthr Cartil*. 2019;27(6):956-964. doi:10.1016/j.joca.2019.01.013
- Mwale F, Roughley P, Antoniou J, et al. Distinction between the extracellular matrix of the nucleus pulposus and hyaline cartilage: a requisite for tissue engineering of intervertebral disc. *Eur Cells Mater*. 2004;8:58-64. doi:10.22203/eCM.v008a06
- Chen JW, Ni BB, Zheng XF, Li B, Jiang SD, Jiang LS. Hypoxia facilitates the survival of nucleus pulposus cells in serum deprivation by Down-regulating excessive autophagy through restricting ROS generation. *Int J Biochem Cell Biol*. 2015;59:1-10. doi:10.1016/j.biocel.2014.11.009
- Zoetebier B, Schmitz TC, Ito K, Karperien M, Tryfonidou MA, Paez JI. Injectable hydrogels for articular cartilage and nucleus pulposus repair: status quo and prospects. *Tissue Eng Part A*. 2022;28(11-12):478-499. doi:10.1089/ten.tea.2021.0226
- de Vries S, van Doeselaar M, Meij B, Tryfonidou M, Ito K. Notochordal cell matrix As a therapeutic agent for intervertebral disc regeneration. *Tissue Eng Part A*. 2019;25(11-12):830-841. doi:10.1089/ten.tea.2018.0026
- Bach FC, Tellegen AR, Beukers M, et al. Biologic canine and human intervertebral disc repair by notochordal cell-derived matrix: from bench towards bedside. *Oncotarget*. 2018;9(41):26507-26526. doi:10.18632/oncotarget.25476
- Schmitz TC, Van Doeselaar M, Tryfonidou MA, Ito K. Detergent-free decellularization of notochordal cell-derived matrix yields a regenerative, injectable, and swellable biomaterial. *ACS Biomater Sci Eng*. 2022;8(9):3912-3923. doi:10.1021/acsbiomaterials.2c00790
- Schmitz TC, Salzer E, Crispim JF, et al. Characterization of biomaterials intended for use in the nucleus pulposus of degenerated intervertebral discs. *Acta Biomater*. 2020;114:1-15. doi:10.1016/j.actbio.2020.08.001
- Ulbricht J, Jordan R, Luxenhofer R. On the biodegradability of polyethylene glycol, Polypeptoids and poly(2-Oxazoline)S. *Biomaterials*. 2014;35(17):4848-4861. doi:10.1016/j.biomaterials.2014.02.029
- Zustiak SP, Leach JB. Hydrolytically degradable poly(ethylene glycol) hydrogel scaffolds with tunable degradation and mechanical properties. *Biomacromolecules*. 2010;11(5):1348-1357. doi:10.1021/bm100137q
- Kroger SM, Hill L, Jain E, et al. Design of Hydrolytically Degradable Polyethylene Glycol Crosslinkers for facile control of hydrogel

- degradation. *Macromol Biosci.* 2020;20(10):1-13. doi:10.1002/mabi.202000085
14. Sivan S-SS, Wachtel E, Tsitron E, et al. Collagen turnover in Normal and degenerate human intervertebral discs as determined by the racemization of aspartic acid. *J Biol Chem.* 2008;283(14):8796-8801. doi:10.1074/jbc.M709885200
  15. Lowinger MB, Barrett SE, Zhang F, Williams RO. Sustained release drug delivery applications of polyurethanes. *Pharmaceutics.* 2018; 10(2):1-19. doi:10.3390/pharmaceutics10020055
  16. Kharkar PM, Rehmann MS, Skeens KM, Maverakis E, Kloxin AM. Thiol-Ene click hydrogels for therapeutic delivery. *ACS Biomater Sci Eng.* 2016;2(2):165-179. doi:10.1021/acsbiomaterials.5b00420
  17. Piazza N, Dehghani M, Gaborski TR, Wuertz-Kozak K. Therapeutic potential of extracellular vesicles in degenerative diseases of the intervertebral disc. *Front Bioeng Biotechnol.* 2020;8(April):1-8. doi:10.3389/fbioe.2020.00311
  18. Bach F, Libregts S, Creemers L, et al. Notochordal-cell derived extracellular vesicles exert regenerative effects on canine and human nucleus pulposus cells. *Oncotarget.* 2017;8(51):88845-88856. doi:10.18632/oncotarget.21483
  19. Trout JJ, Buckwalter JA, Moore KC, Landas SK. Ultrastructure of the human intervertebral disc. I. Changes in notochordal cells with age. *Tissue Cell.* 1982;14(2):359-369. doi:10.1016/0040-8166(82)90033-7
  20. Richardson SM, Ludwinski FE, Gnanalingham KK, Atkinson RA, Freemont AJ, Hoyland JA. Notochordal and nucleus pulposus marker expression is maintained by sub-populations of adult human nucleus pulposus cells through aging and degeneration. *Sci Rep.* 2017;7(1): 1501. doi:10.1038/s41598-017-01567-w
  21. Sakai D, Nakamura Y, Nakai T, et al. Exhaustion of nucleus pulposus progenitor cells with ageing and degeneration of the intervertebral disc. *Nat Commun.* 2012;3(1):1264. doi:10.1038/ncomms2226
  22. Platt JL, Cascalho M, Piedrahita JA. Xenotransplantation: Progress along paths uncertain from models to application. *ILAR J.* 2018;59(3): 286-308. doi:10.1093/ilar/ily015
  23. Hu S, Xing H, Zhang J, et al. Mesenchymal stem cell-derived extracellular vesicles: immunomodulatory effects and potential applications in intervertebral disc degeneration. *Stem Cells Int.* 2022;2022:1-13. doi: 10.1155/2022/7538025
  24. Binch ALA, Fitzgerald JC, Growney EA, Barry F. Cell-based strategies for IVD repair: clinical Progress and translational obstacles. *Nat Rev Rheumatol.* 2021;17(3):158-175. doi:10.1038/s41584-020-00568-w
  25. Gilchrist CL, Darling EM, Chen J, Setton LA. Extracellular matrix ligand and stiffness modulate immature nucleus pulposus cell-cell interactions. *PLoS One.* 2011;6(11):e27170. doi:10.1371/journal.pone.0027170
  26. Humphreys MD, Ward L, Richardson SM, Hoyland JA. An optimized culture system for notochordal cell expansion with retention of phenotype. *JOR Spine.* 2018;1(3):1-14. doi:10.1002/jsp2.1028
  27. Thorpe AA, Bach FC, Tryfonidou MA, et al. Leaping the hurdles in developing regenerative treatments for the intervertebral disc from preclinical to clinical. *JOR Spine.* 2018;1(3):e1027. doi:10.1002/jsp2.1027
  28. Wall A, Board T. A direct spectrophotometric microassay for sulphated glycosaminoglycans in cartilage cultures. *Class Pap Orthop.* 2014;9:431-432. doi:10.1007/978-1-4471-5451-8\_109
  29. Hofmann S, Hagenmüller H, Koch AM, et al. Control of in vitro tissue-engineered bone-like structures using human mesenchymal stem cells and porous silk scaffolds. *Biomaterials.* 2007;28(6):1152-1162. doi:10.1016/j.biomaterials.2006.10.019
  30. Williams RJ, Tryfonidou MA, Snuggs JW, Le Maitre CL. Cell sources proposed for nucleus pulposus regeneration. *JOR Spine.* 2021;4(4):1-27. doi:10.1002/jsp2.1175
  31. U.S. Department of Health and Human Services; Food and Drug Administration. Content and review of chemistry, manufacturing, and control (CMC) information for human somatic cell therapy investigational new drug applications (INDs). Guidance for FDA reviewers and sponsors 2008, 1-36.
  32. Salvatierra JC, Yuan TY, Fernando H, et al. Difference in energy metabolism of annulus fibrosus and nucleus pulposus cells of the intervertebral disc. *Cell Mol Bioeng.* 2011;4(2):302-310. doi:10.1007/s12195-011-0164-0
  33. Tavana S, Prior J, Baxan N, et al. Internal deformations in human intervertebral discs under axial compression: a 9.4T MRI study. *Spine J.* 2019;19(9):S51-S52. doi:10.1016/j.spinee.2019.05.120
  34. Almawash S, Osman SK, Mustafa G, El Hamd MA. Current and future prospective of injectable hydrogels—design challenges and limitations. *Pharmaceutics.* 2022;15(3):371. doi:10.3390/ph15030371
  35. Causa F, Manto L, Borzacchiello A, et al. Spatial and structural dependence of mechanical properties of porcine intervertebral disc. *J Mater Sci Mater Med.* 2002;13(12):1277-1280. doi:10.1023/A:1021143516436
  36. Johannessen W, Elliott DM. Effects of degeneration on the biphasic material properties of human nucleus pulposus in confined compression. *Spine.* 2005;30(24):E724-E729.
  37. Iatridis JC, Setton LA, Weidenbaum M, Mow VC. Alterations in the mechanical behavior of the human lumbar nucleus pulposus with degeneration and aging. *J Orthop Res.* 1997;15(2):318-322. doi:10.1002/jor.1100150224
  38. Freemont AJ. The cellular pathobiology of the degenerate intervertebral disc and discogenic Back pain. *Rheumatology.* 2009;48(1):5-10. doi:10.1093/rheumatology/ken396
  39. Sivan SS, Wachtel E, Roughley P. Structure, function, aging and turnover of aggrecan in the intervertebral disc. *Biochim Biophys Acta - Gen Subj.* 2014;1840(10):3181-3189. doi:10.1016/j.bbagen.2014.07.013
  40. Thompson DG, Osborn JC, Kober EM, Schoonover JR. Effects of hydrolysis-induced molecular weight changes on the phase separation of a polyester polyurethane. *Polym Degrad Stab.* 2006;91(12): 3360-3370. doi:10.1016/j.polydegradstab.2006.05.019
  41. Mondal S, Martin D. Hydrolytic degradation of segmented polyurethane copolymers for biomedical applications. *Polym Degrad Stab.* 2012;97(8):1553-1561. doi:10.1016/j.polydegradstab.2012.04.008
  42. Tan RYH, Lee CS, Pichika MR, Cheng SF, Lam KY. PH responsive polyurethane for the advancement of biomedical and drug delivery. *Polymers.* 2022;14(9):1672. doi:10.3390/polym14091672
  43. Power KA, Grad S, Rutges JPHJ, et al. Identification of cell surface-specific markers to target human nucleus pulposus cells: expression of carbonic anhydrase XII varies with age and degeneration. *Arthritis Rheum.* 2011;63(12):3876-3886. doi:10.1002/art.30607
  44. Silagi ES, Schoepflin ZR, Seifert EL, et al. Bicarbonate recycling by HIF-1-dependent carbonic anhydrase isoforms 9 and 12 is critical in maintaining intracellular PH and viability of nucleus pulposus cells. *J Bone Miner Res.* 2018;33(2):338-355. doi:10.1002/jbmr.3293
  45. Jia H, Huang Z, Li Z, Zheng Z, Wang X. One-pot synthesis of highly mechanical and redox-degradable polyurethane hydrogels based on tetra-PEG and Disulfide/thiol chemistry. *RSC Adv.* 2016;6(54):48863-48869. doi:10.1039/C6RA04320H
  46. Kim E, Yang J, Choi J, Suh J-S, Huh Y-M, Haam S. Synthesis of gold nanorod-embedded polymeric nanoparticles by a nanoprecipitation method for use as photothermal agents. *Nanotechnology.* 2009; 20(36):365602. doi:10.1088/0957-4484/20/36/365602
  47. Park Y, Lutolf MP, Hubbell JA, Hunziker EB, Wong M. Bovine primary chondrocyte culture in synthetic matrix metalloproteinase-sensitive poly(ethylene glycol)-based hydrogels as a scaffold for cartilage repair. *Tissue Eng.* 2004;10(3-4):515-522. doi:10.1089/107632704323061870



48. Patterson J, Hubbell JA. Enhanced proteolytic degradation of molecularly engineered PEG hydrogels in response to MMP-1 and MMP-2. *Biomaterials*. 2010;31(30):7836-7845. doi:10.1016/j.biomaterials.2010.06.061
49. Jha AK, Tharp KM, Browne S, et al. Matrix Metalloproteinase-13 mediated degradation of hyaluronic acid-based matrices orchestrates stem cell engraftment through vascular integration. *Biomaterials*. 2016;89:136-147. doi:10.1016/j.biomaterials.2016.02.023
50. Stewart SA, Coulson MB, Zhou C, Burke NAD, Stöver HDH. Synthetic hydrogels formed by thiol-Ene crosslinking of vinyl sulfone-functional poly(methyl vinyl ether-*alt*-maleic acid) with  $\alpha$ ,  $\omega$ -Dithio-Polyethyleneglycol. *Soft Matter*. 2018;14(41):8317-8324. doi:10.1039/c8sm01066h
51. Nachemson A. Intradiscal measurements of PH in patients with lumbar rhizopathies. *Acta Orthop Scand*. 1969;40(1):23-42. doi:10.3109/17453676908989482
52. Paez J, Farrukh A, Włodarczyk-Biegun MK, del Campo A. *Thiol-Methylsulfone Based Hydrogels: Enhanced Control on Gelation Kinetics for 3D Cell Encapsulation*; 2019. doi:10.26434/chemrxiv.8971136.v1
53. Hammer N, Brandl FP, Kirchof S, Messmann V, Goepferich AM. Protein compatibility of selected cross-linking reactions for hydrogels. *Macromol Biosci*. 2015;15(3):405-413. doi:10.1002/mabi.201400379
54. Kirschner CM, Anseth KS. Hydrogels in healthcare: from static to dynamic material microenvironments. *Acta Mater*. 2013;61(3):931-944. doi:10.1016/j.actamat.2012.10.037
55. Lüsse S, Arnold K. The interaction of poly(ethylene glycol) with water studied by 1H and 2H NMR relaxation time measurements. *Macromolecules*. 1996;29(12):4251-4257. doi:10.1021/ma9508616
56. Bach FC, de Vries SAH, Riemers FM, et al. Soluble and Pelletable factors in porcine, canine and human notochordal cell-conditioned medium: implications for IVD regeneration. *Eur Cells Mater*. 2016;32:163-180. doi:10.22203/eCM.v032a11
57. DiStefano TJ, Vaso K, Danias G, Chionuma HN, Weiser JR, Iatridis JC. Extracellular vesicles as an emerging treatment option for intervertebral disc degeneration: therapeutic potential, translational pathways, and regulatory considerations. *Adv Healthc Mater*. 2022;11(5):2100596. doi:10.1002/adhm.202100596
58. Omlor GW, Nerlich AG, Tirlapur UK, Urban JP, Guehring T. Loss of notochordal cell phenotype in 3D-cell cultures: implications for disc physiology and disc repair. *Arch Orthop Trauma Surg*. 2014;134:1673-1681. doi:10.1007/s00402-014-2097-2
59. Panebianco CJ, Meyers JH, Gansau J, Hom WW, Iatridis JC. Balancing biological and biomechanical performance in intervertebral disc repair: a systematic review of injectable cell delivery biomaterials. *Eur Cell Mater*. 2020;40:239-258. doi:10.22203/eCM.v040a15
60. Bach FC, Poramba-Liyanage DW, Riemers FM, et al. Notochordal cell-based treatment strategies and their potential in intervertebral disc regeneration. *Front Cell Dev Biol*. 2022;9:1-23. doi:10.3389/fcell.2021.780749
61. Hunter CJ, Matyas JR, Duncan NA. The functional significance of cell clusters in the notochordal nucleus pulposus: survival and signaling in the canine intervertebral disc. *Spine*. 2004;29(10):1099-1104. doi:10.1097/00007632-200405150-00010
62. Spillekom S, Smolders LA, Grinwis GCM, et al. Increased osmolarity and cell clustering preserve canine notochordal cell phenotype in culture. *Tissue Eng-Part C Methods*. 2014;20(8):652-662. doi:10.1089/ten.tec.2013.0479
63. Colombier P, Halgand B, Chédeville C, et al. NOTO transcription factor directs human induced pluripotent stem cell-derived Mesoderm progenitors to a notochordal fate. *Cell*. 2020;9(2):509. doi:10.3390/cells9020509
64. Zhang Y, Zhang Z, Chen P, et al. Directed differentiation of notochord-like and nucleus pulposus-like cells using human pluripotent stem cells. *Cell Rep*. 2020;30(8):2791-2806.e5. doi:10.1016/j.celrep.2020.01.100
65. Liu Y, Fu S, Rahaman MN, Mao JJ, Bal BS. Native nucleus pulposus tissue matrix promotes notochordal differentiation of human induced pluripotent stem cells with potential for treating intervertebral disc degeneration. *J Biomed Mater Res-A*. 2015;103(3):1053-1059. doi:10.1002/jbm.a.35243

## SUPPORTING INFORMATION

Additional supporting information can be found online in the Supporting Information section at the end of this article.

**How to cite this article:** Schmitz TC, van Genabeek B, Pouderoijen MJ, et al. Semi-synthetic degradable notochordal cell-derived matrix hydrogel for use in degenerated intervertebral discs: Initial in vitro characterization. *J Biomed Mater Res*. 2023;111(12):1903-1915. doi:10.1002/jbm.a.37594